Title

Discovery and Genomic Characterization of a Novel Henipavirus, Angavokely Virus, from Fruit Bats in Madagascar

Journal

Journal of Virology, 96(18)

ISSN

0022-538X

Authors

Madera, Sharline
Kistler, Amy
Ranaivoson, Hafaliana C
et al.

Publication Date

2022-09-28

DOI

10.1128/jvi.00921-22

Peer reviewed

AMERICAN SOCIETY FOR MICROBIOLOGY | Journal of Virology®

GENETIC DIVERSITY AND EVOLUTION

Discovery and Genomic Characterization of a Novel Henipavirus, Angavokely Virus, from Fruit Bats in Madagascar

Sharline Madera,[a] Amy Kistler,[b] Hafaliana C. Ranaivoson,[c,d,e] Vida Ahyong,[b] Angelo Andrianiaina,[e] Santino Andry,[f] Vololoniaina Raharinosy,[d] Tsiry H. Randriambolamanantsoa,[d] Ny Anjara Fifi Ravelomanantsoa,[e] Cristina M. Tato,[b] Joseph L. DeRisi,[b,g] Hector C. Aguilar,[h] Vincent Lacoste,[d] Philippe Dussart,[d] Jean-Michel Heraud,[d,i] Cara E. Brook[c]

[a]Division of Infectious Diseases, Department of Medicine, University of California, San Francisco, California, USA
[b]Chan Zuckerberg Biohub, San Francisco, California, USA
[c]Department of Ecology and Evolution, University of Chicago, Chicago, Illinois, USA
[d]Virology Unit, Institut Pasteur de Madagascar, Antananarivo, Madagascar
[e]Department of Zoology and Animal Biodiversity, University of Antananarivo, Antananarivo, Madagascar
[f]Department of Entomology, University of Antananarivo, Antananarivo, Madagascar
[g]Department of Medicine and Biochemistry & Biophysics, University of California, San Francisco, California, USA
[h]Department of Microbiology and Immunology, College of Veterinary Medicine, Cornell University, Ithaca, New York, USA
[i]Virology Department, Institut Pasteur de Dakar, Dakar, Senegal

ABSTRACT The genus *Henipavirus* (family *Paramyxoviridae*) currently comprises seven viruses, four of which have demonstrated prior evidence of zoonotic capacity. These include the biosafety level 4 agents Hendra (HeV) and Nipah (NiV) viruses, which circulate naturally in pteropodid fruit bats. Here, we describe and characterize Angavokely virus (AngV), a divergent henipavirus identified in urine samples from wild, Madagascar fruit bats. We report the nearly complete 16,740-nucleotide genome of AngV, which encodes the six major henipavirus structural proteins (nucleocapsid, phosphoprotein, matrix, fusion, glycoprotein, and L polymerase). Within the phosphoprotein (P) gene, we identify an alternative start codon encoding the AngV C protein and a putative mRNA editing site where the insertion of one or two guanine residues encodes, respectively, additional V and W proteins. In other paramyxovirus systems, C, V, and W are accessory proteins involved in antagonism of host immune responses during infection. Phylogenetic analysis suggests that AngV is ancestral to all four previously described bat henipaviruses—HeV, NiV, Cedar virus (CedV), and Ghanaian bat virus (GhV)—but evolved more recently than rodent- and shrew-derived henipaviruses, Mojiang (MojV), Gamak (GAKV), and Daeryong (DARV) viruses. Predictive structure-based alignments suggest that AngV is unlikely to bind ephrin receptors, which mediate cell entry for all other known bat henipaviruses. Identification of the AngV receptor is needed to clarify the virus's potential host range. The presence of V and W proteins in the AngV genome suggest that the virus could be pathogenic following zoonotic spillover.

IMPORTANCE Henipaviruses include highly pathogenic emerging zoonotic viruses, derived from bat, rodent, and shrew reservoirs. Bat-borne Hendra (HeV) and Nipah (NiV) are the most well-known henipaviruses, for which no effective antivirals or vaccines for humans have been described. Here, we report the discovery and characterization of a novel henipavirus, Angavokely virus (AngV), isolated from wild fruit bats in Madagascar. Genomic characterization of AngV reveals all major features associated with pathogenicity in other henipaviruses, suggesting that AngV could be pathogenic following spillover to human hosts. Our work suggests that AngV is an ancestral bat henipavirus that likely uses viral entry pathways distinct from those previously described for HeV and NiV. In Madagascar, bats are consumed as a source of human food, presenting opportunities for cross-species transmission. Characterization of novel henipaviruses and documentation of

Editor Anice C. Lowen, Emory University School of Medicine

Address correspondence to Cara E. Brook, cbrook@uchicago.edu.

The authors declare no conflict of interest.

Received 23 June 2022
Accepted 10 August 2022
Published 30 August 2022

their pathogenic and zoonotic potential are essential to predicting and preventing the emergence of future zoonoses that cause pandemics.

KEYWORDS emerging zoonosis, henipavirus, novel virus, *Eidolon dupreanum*, bat-borne virus, Madagascar

Henipaviruses (HNVs) belong to a genus of bat-, rodent-, and shrew-borne viruses within the family *Paramyxoviridae* with demonstrated zoonotic potential. HNVs can manifest extreme virulence in human hosts, as exemplified by the prototypical HNVs, Hendra virus (HeV), and Nipah virus (NiV), which cause severe acute respiratory distress and/or encephalitis in humans, yielding case fatality rates that can exceed 90% (1 to 3). This high pathogenicity and the lack of approved HNV therapeutics or vaccines for humans have garnered HeV and NiV classification as Biological Safety Level 4 (BSL4) agents and WHO priority diseases. Since their discovery in the 1990s, HeV and NiV have periodically spilled over to humans from their reservoir hosts, pteropodid bats. HeV zoonosis is mediated by spillover to intermediate horse hosts, from which humans acquire infection (4). NiV can spillover to humans via intermediate transmission through pig hosts, or directly from bat to human, resulting in near-annual outbreaks of fatal encephalitis in South Asia, where subsequent human-to-human transmission also occurs (2, 5 to 7).

Novel HNVs continue to emerge from wildlife hosts and represent ongoing threats to human health. Initially, the *Henipavirus* genus comprised only HeV and NiV; however, the last 2 decades have witnessed the discovery of five new HNVs: bat-borne Cedar virus (CedV) and Ghanaian bat virus (GhV), rodent-borne Mojiang virus (MojV), and shrew-borne Gamak (GAKV) and Daeryong viruses (DARV) (8 to 11). News of an eighth putative henipavirus—and the fifth recognized zoonotic HNV—came to light while this article was in press: Langya henipavirus (LayV), a close relative of MojV, was recently identified in febrile patients in eastern China (12). Of these novel HNVs, at least three show evidence of zoonotic potential: serological data suggest prior human exposure to GhV or to an antigenically related virus in West Africa (13), while MojV was first identified following a human outbreak of severe pneumonia in Chinese mine workers, all of whom died after infection (9). Additionally, LayV was first identified in part with sentinel surveillance of human febrile patients with a history of animal contact, then later found to circulate at high seroprevalence in shrews (12). Thus, in addition to their high potential for pathogenicity, HNVs possess a broad host range that spans at least seven mammalian orders, including bats (10, 14).

Cross-species viral spillover necessitates effective interspecies transmission, which first requires a virus to successfully enter the cells of diverse host species. In general, HNVs use the highly conserved ephrin family of proteins, both type A and type B, as cell entry receptors (1, 8, 15 to 17). A notable exception to this pattern is MojV, which does not use ephrin proteins—or the sialic acid and CD150 receptors common to non-HNV paramyxoviruses—to gain cell entry (15, 18). Indeed, as of yet, the viral entry receptor for MojV—and the closely related GAKV, DARV, and LayV—remain unknown. In general, viruses in the genus *Henipavirus* have broad host ranges and cause high case fatality rates following human spillover, making the characterization of new HNVs a high public health priority.

The HNV genome consists of six structural proteins: nucleocapsid (N), phosphoprotein (P), matrix (M), fusion (F), glycoprotein (G), and polymerase (L). In comparison with other members of the family *Paramyxoviridae*, HNVs have relatively larger genomes (approximately 18 kb versus 16 kb). This extended length is largely due to several, long 3′ untranslated regions (UTRs) of the N, P, F and G mRNAs (19, 20). The genome length of HNVs, like all paramyxoviruses, adheres to the so-called "rule of six," whereby viral genomes consistently demonstrate polyhexameric length (21). The "rule of six" is believed to be a requirement for efficient genome replication under the unique mRNA editing features of the paramyxovirus genome (21). The paramyxovirus P locus exhibits notable transcription properties that are shared across most members of the *Paramyxoviridae* family. The P gene permits the translation of additional

accessory proteins from either gene editing events within the locus (prior to translation) or an overlapping open reading frame (ORF) in the P gene itself. All HNVs, with the exception of CedV, harbor a highly conserved mRNA editing site at which the insertion of additional guanine residues can result in the translation of accessory proteins, V and W, involved in viral antagonism and evasion of the host immune system (1). The HNV P gene also contains an overlapping ORF that allows for the synthesis of a third accessory protein, C, which is also involved in viral host immune evasion (1).

Our lab has previously presented evidence of exposure to henipa-like viruses in serum collected from three endemic Madagascar fruit bat species (*E. dupreanum*, *Pteropus rufus*, and *Rousettus madagascariensis*) using a Luminex serological assay that identified cross-reactivity to CedV/NiV/HeV-G and -F proteins (22). The most significant antibody binding previously detected corresponded to the NiV-G antigen for *E. dupreanum* serum and the HeV-F antigen for *P. rufus* and *R. madagascariensis* serum, suggesting the potential circulation of multiple HNVs in the Madagascar fruit bat system (22). Fruit bats, including *E. dupreanum*, are consumed widely in Madagascar as a source of human food, presenting opportunities for cross-species zoonotic emergence. This underscores the importance of further characterization of the pathogenic and zoonotic potential of potential HNVs circulating in the Madagascar fruit bat system. Here, we describe and characterize a novel bat HNV genome, Angavokely virus (AngV), recovered from urine samples collected from the Madagascar fruit bat, *E. dupreanum*. Our work suggests AngV is part of an ancestral group of HNVs that may rely on a novel, non-ephrin-mediated viral entry pathway.

RESULTS

Discovery and prevalence of HNV in Malagasy bats. Urine swab specimens from 206 bats were collected in 8 roosting sites across the island of Madagascar from 2013 to 2019 (Fig. 1). Urine samples were collected during wet and dry seasons from all three Madagascar fruit bat species, *P. rufus*, *E. dupreanum*, and *R. madagascariensis* (Table 1). Isolated RNA from urine swab specimens generated an average of 19 million paired-read sequences. In total, 10/206 (4.9%) bats were positive for HNV; all positive samples were collected from *E. dupreanum* bats (10/106; 9.4%) at the Angavokely cave roosting site (Table 1). Positive samples were collected in wet and dry seasons from both male and female adults.

Genomic characterization of AngV. We recovered one near-full-length HNV contig (16,740 nucleotides [nt]), supported by an average sequencing depth of 14 reads (Fig. 2A), from a urine sample collected from an adult, nonlactating *E. dupreanum* female in the 2018–2019 wet season (capture date: 15 March 2019). We focused subsequent genomic analyses on this longest sequence, which we named Angavokely virus (AngV) after the site of *E. dupreanum* capture.

As with other members of the *Henipavirus* genus, the genome of AngV is organized into 6 open reading frames (ORFs) arranged in the order 3′-N-P-M-F-G-L-5′. AngV shares an average nucleotide identity of 36% with the NiV reference genome (AF212302) and a varying amino acid identity that is highest across the ORFs encoding the nucleocapsid and L polymerase proteins (Fig. 2B and C).

AngV coding regions. The P gene of AngV follows an organization similar to most members of the *Henipavirus* genus. AngV harbors alternative start sites that, respectively, encode the P and C proteins, as well as a conserved putative mRNA editing site common to most paramyxoviruses $A^{4\text{-}6}G^{2\text{-}3}$ (Fig. 3A and B). AngV shares an identical putative mRNA editing site with the recently discovered HNVs, MojV and GAKV. Pseudotemplated addition of one or two G residues at the conserved putative mRNA editing site generates a putative V and W protein, respectively (Fig. 3C; W protein in Fig. S1 in the supplemental material). In congruence with members of the *Henipavirus* genus that encode the conserved putative mRNA editing site, the putative V protein of AngV harbors a unique C-terminal region that contains a highly conserved cysteine-rich zinc finger domain (Fig. 3C).

The length of each ORF in the AngV genome resembles those from previously described HNVs, with the exception of the gene encoding the glycoprotein (G)—which, at 688 amino

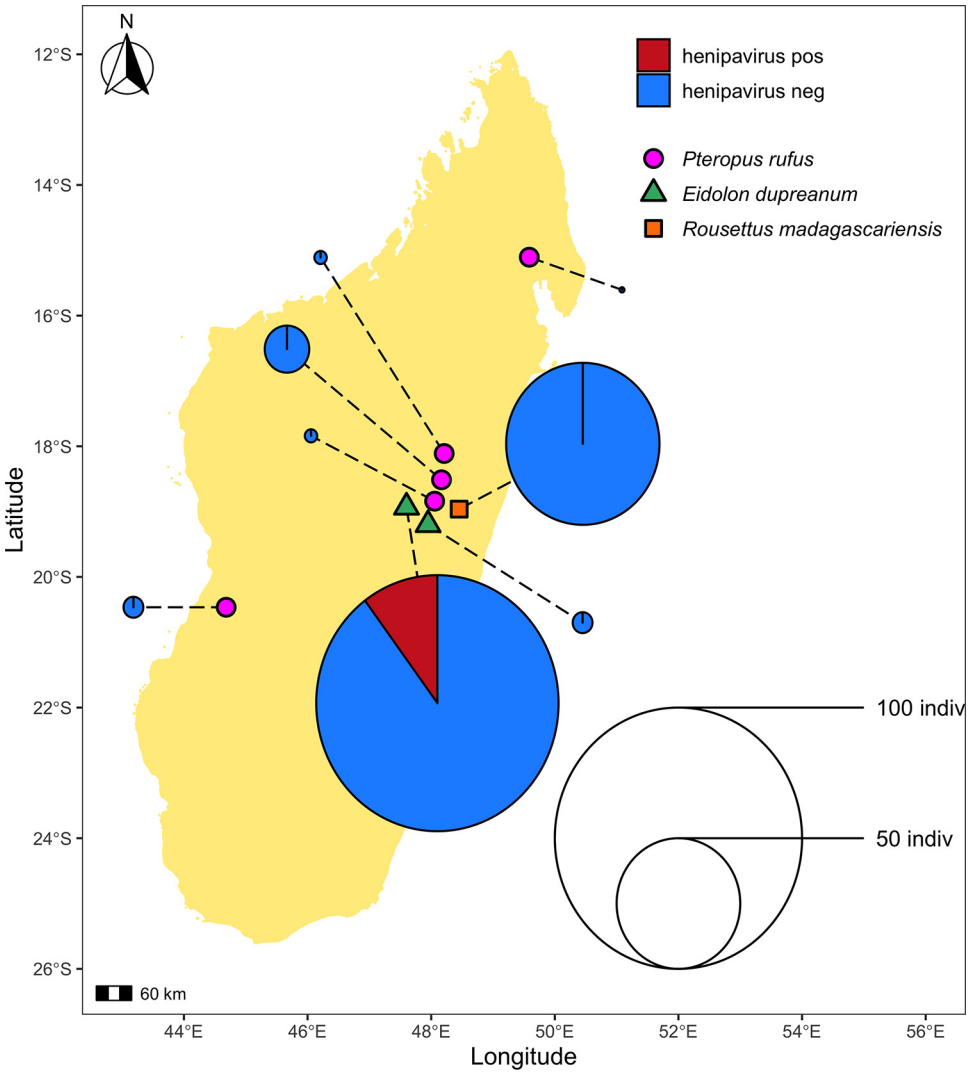

FIG 1 Geographic location of sampling sites used in this study. Sampling sites grouped by bat species found depicted as follows: *P. rufus* (pink circles) Ambakoana (−18.51 S, 48.17 E)/Mahabo (−20.46 S, 44.68 E)/Mahialambo (−18.11 S, 48.21 E)/Makira (−15.11 S, 49.59 E)/Marovitsika (−18.84 S, 48.06 E) roosts; *E. dupreanum* (green triangles) Angavobe (−18.94 S, 47.95 E)/Angavokely (−18.93 S, 47.76 E) caves; *R. madagascariensis* (orange squares) Maromizaha cave (−18.96 S, 48.45). Dashed lines link each sampling site to corresponding pie charts, which show the percentage of HNV-positive specimens for all sampled species and sites. Dashed lines are included for visualization purposes only, and variation in length is not significant. Pies are size-weighted by the total bat population sampled at each site, corresponding to the legend. HNV-positive samples were only recovered from the *E. dupreanum* Angavokely site.

acids (aa), is 56 aa longer than the longest previously characterized HNV glycoprotein from GhV (632 aa; Table 2) (16). BLAST analysis indicates that AngV ORFs for genes encoding the nucleocapsid (N), matrix (M), and polymerase (L) proteins exhibit the highest nucleotide and amino acid pairwise identity with other HNVs, with highest similarity shared with the NiV L protein (nt 74.7%, aa 52.2%, Table 2). In contrast to many emerging viruses, AngV largely exhibits higher nucleotide versus amino acid identity with other HNVs (Table 2). The more recently discovered HNVs (MojV, CedV, GAKV, DARV, GhV) mirror this pattern, showing higher nucleotide versus amino acid identity compared to NiV and HeV (data not shown).

AngV noncoding regions. Examination of all viral intergenic regions (in cRNA orientation) reveals that AngV exhibits the highly conserved CTT intergenic junction site characteristic of other HNVs, as well as gene stop and gene start sites with high similarity to those of previously described HNVs (Table S1). We were unable to locate the intergenic junction site and transcriptional start or stop site in the 5′ region of the N

TABLE 1 Prevalence of HNV infections in the urine of Malagasy bats captured during 2013–2019 collection period

		By site		By season/sex		
Roost site	Species	Total sampled	Total henipavirus positive	Season	Total sampled # (M, F)	Total henipavirus positive # (M, F)
Ambakoana	*P. rufus*	18	0	wet '13	2 (1, 1)	0 (0, 0)
				wet '14/'15	3 (3, 0)	
				wet '15/'16	2 (2, 0)	
				wet '17/'18	2 (2, 0)	
				wet '18/'19	9 (6, 3)	
Angavobe	*E. dupreanum*	8	0	wet '17/'18	5 (1, 4)	0 (0, 0)
				dry '18	3 (1, 2)	0 (0, 0)
Angavokely	*E. dupreanum*	98	10	wet '15/'16	2 (1, 1)	0 (0, 0)
				wet '17/'18	38 (5, 33)	4 (0, 4)
				dry '18	11 (8, 3)	2 (1, 1)
				wet '18/'19	47 (20, 27)	4 (2, 2)
Mahabo	*P. rufus*	8	0	dry '14	8 (4, 4)	0 (0, 0)
Mahialambo	*P. rufus*	5	0	wet '18/'19	5 (2, 3)	0 (0, 0)
Makira	*P. rufus*	2	0	dry '15	2 (2, 0)	0 (0, 0)
Marovitsika	*P. rufus*	62	0	wet '17/'18	9 (3, 6)	0 (0, 0)
				dry '18	7 (3, 4)	
				wet '18/'19	46 (20, 26)	
Maromizaha	*R. madagascariensis*	5	0	wet '13	2 (1, 1)	0 (0, 0)
				dry '14	1 (0, 1)	
				wet '14/'15	2 (2, 0)	

ORF for AngV, suggesting that the genomic 3′ untranslated regions (UTRs) for AngV have not yet been fully recovered. Comparison of the 5′ and 3′ UTRs for AngV with those of other HNVs reveals UTRs of varying lengths within the *Henipavirus* genus (Table S2). Nevertheless, AngV exhibits similar lengths and a nucleotide identity of roughly 30 to 40% for the 5′ and 3′ UTRs of most HNV genes; however, the P gene 3′

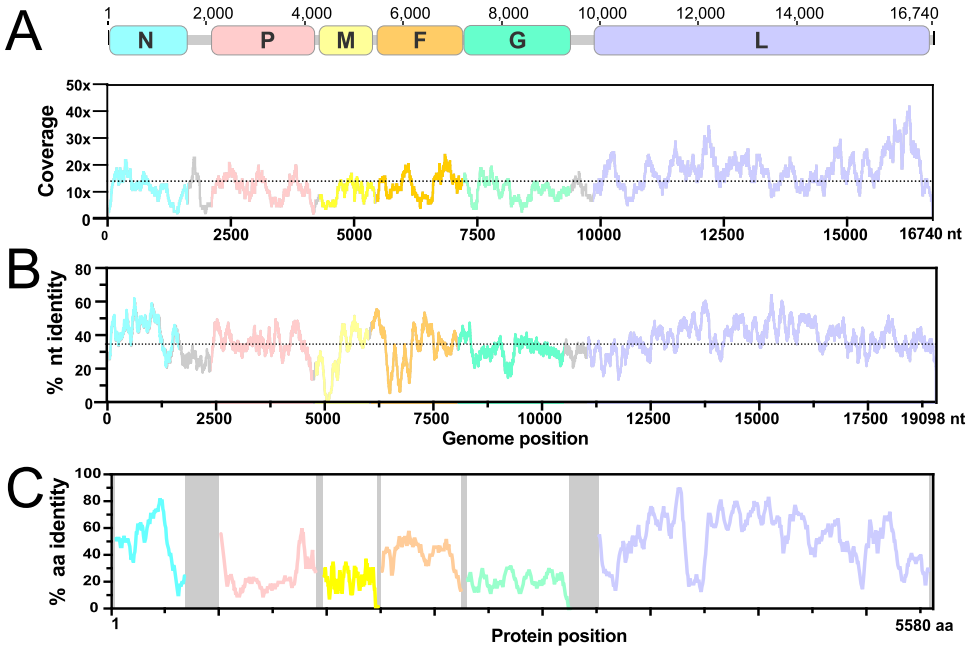

FIG 2 AngV genome organization. (A) Coding regions for each gene are shown and depicted in color; noncoding intergenic and terminal regions are highlighted in gray. Depicted genes represented as follows: nucleocapsid (N), phosphoprotein (P), matrix (M), fusion (F), glycoprotein (G), and RNA polymerase (L). Sequencing read depth supporting each position of the recovered genome sequence is plotted below the genomic schematic. Scanning nucleotide (B) and amino acid (C) pairwise identity to Nipah virus (GenBank accession number: AF212302). Dotted horizontal lines represent average read depth (14.29) or average nucleotide pairwise identity (36%).

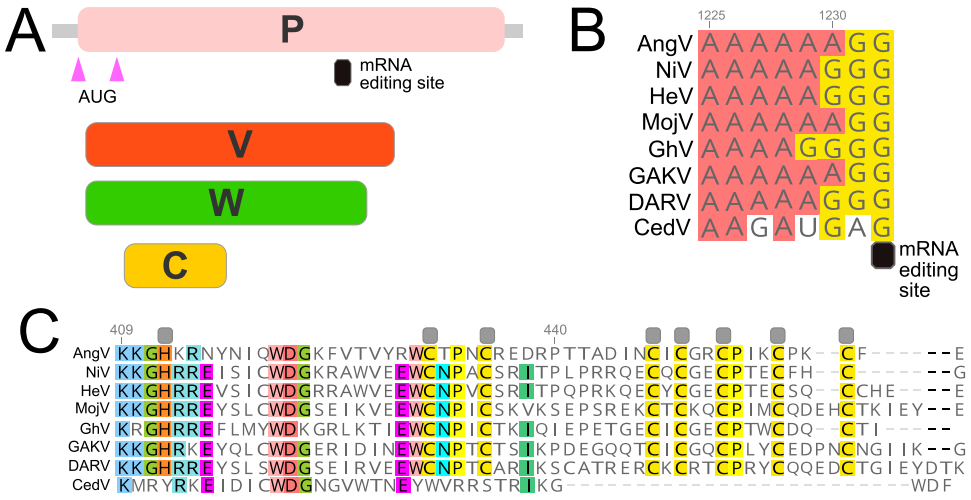

FIG 3 Organization of the P gene of AngV. (A) Alternative transcriptional start sites (pink triangle) generate the P and C protein. Pseudotemplated addition of one or two guanine nucleotides at the putative mRNA editing site generates a V and W protein, respectively. (B) Sequence alignment of the putative mRNA editing site across members of the *Henipavirus* genus (cRNA depicted). (C) Amino acid alignment of the unique C-terminal region of the V protein following the addition of one guanine nucleotide to the putative mRNA editing site. Gray boxes denote conserved cysteine and histidine residues suggested to directly coordinate bound zinc ions (32). Individual nucleotides or amino acids are color coordinated if at least 75% conserved at the alignment position. Nucleotide or amino acid position numbers displayed represent the position within the AngV gene or protein. Virus name (abbreviation), followed by GenBank accession number: Angavokely virus (AngV) ON613535; Nipah virus (NiV) AF212302; Hendra virus (HeV) AF017149; Mojiang virus (MojV) KF278639; Ghanaian bat Henipavirus (GhV) HQ660129; Daeryong virus (DARV) MZ574409; Gamak virus (GAKV) MZ574407; Cedar virus (CedV) JQ001776. CedV is shown here only for comparison, as the CedV P protein is not believed to undergo RNA editing or to generate a functional V protein (8, 32).

UTR, the M gene 5′ and 3′ UTRs, and the F gene 5′ and 3′ UTRs are significantly shorter in AngV compared with previously described HNVs. Correspondingly, nucleotide identity varies when comparing this shorter subset of 5′ and 3′ UTRs for AngV against other HNVs (Table S2).

Phylogenetic analyses. Phylogenetic analysis of complete L protein amino acid sequences across the *Paramyxoviridae* family places AngV within the *Henipavirus* genus at <0.82 nucleotide substitutions away from the node distinguishing the family *Paramyxoviridae* from the *Sunviridae* (Fig. 4A). AngV clusters independently within the *Henipavirus* genus and diverges ancestral to all currently known bat-borne HNVs. Our time-resolved Bayesian phylogeny further corroborates this result, placing AngV ancestral to all previously described bat-borne HNVs but more recently diverged than the rodent- and shrew-borne HNVs, MojV, GAKV, and DARV (Fig. 4B; Fig. S2). We estimate the divergence of the AngV lineage from the rest of the HNV clade at 9,794 years ago (95% highest posterior density [HPD] 6,519 to 14,024 years), and the time to the most recent common ancestor (MRCA) for the entire HNV genus as 11,195 years ago (95% HPD 7,351 to 15,905 years).

TABLE 2 Length and pairwise sequence identity of predicted open reading frames of AngV and other HNV

Gene	AngV length aa	NiV length aa (%nt, %aa)	HeV	MojV	CedV	GAKV	DARV	GhV
N	514	532 (56.4, 48.0)	532 (55.4, 46.7)	539 (55.8, 45.3)	510 (57.5, 48.3)	533 (58.0, 47.5)	574 (55.3, 24.0)	514 (56.2, 48.9)
P	693	709 (47.8, 25.1)	707 (48.1, 24.1)	694 (47.6, 23.6)	737 (42.3, 21.6)	586 (43.8, 22.5)	698 (47.3, 23.2)	870 (42.2, 23.1)
C	173	166 (51.3, 25.7)	166 (51.5, 25.1)	177 (47.6, 22.5)	177 (54.5, 29.8)	184 (47.4, 27.5)	175 (48.1, 24.0)	163 (46.1, 23.1)
V	461	456 (46.9, 22.8)	457 (48.5, 23.6)	464 (47.2, 24.5)		370 (43.0, 22.3)	468 (47.2, 22.2)	621 (24.7, 19.8)
W	412	450 (47.0, 21.3)	448 (45.0, 20.0)	435 (46.5, 22.5)		331 (43.9, 22.7)	437 (45.5, 21.1)	572 (39.3, 16.8)
M	354	352 (60.0, 54.6)	352 (59.5, 54.0)	340 (57.1, 53.4)	360 (56.9, 53.1)	340 (56.1, 50.8)	345 (56.5, 52.3)	343 (56.9, 51.4)
F	539	546 (53.7, 39.4)	546 (51.7, 39.4)	545 (52.2, 40.6)	557 (51.8, 36.3)	565 (53.3, 39.4)	545 (58.8, 40.1)	662 (45.5, 35.4)
G	688	602 (43.5, 21.4)	604 (43.8, 20.4)	625 (43.0, 21.2)	622 (43.3, 19.8)	635 (44.9, 17.8)	628 (44.3, 18.7)	632 (42.5, 19.8)
L	2,259	2,244 (74.7, 52.2)	2,244 (57.6, 51.9)	2,277 (57.5, 51.8)	2,501 (52.4, 44.8)	2,291 (57.7, 51.0)	2,271 (58.8, 51.3)	2,250 (57.0, 49.1)

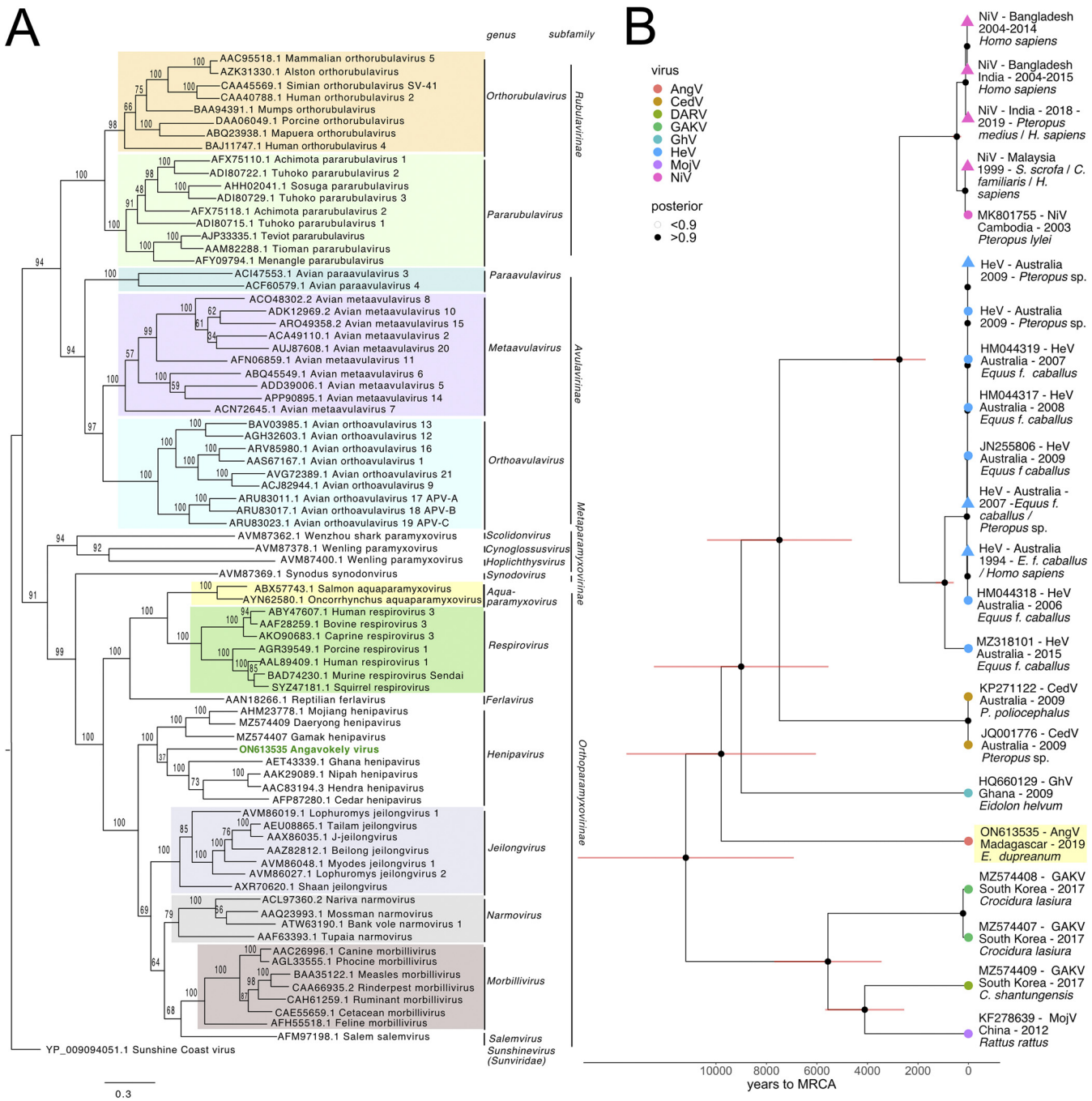

FIG 4 (A) Phylogenetic analysis of the complete L protein sequences of members of the family *Paramyxoviridae*. We note that the sequence for the newly described Langya henipavirus (LayV) (12) was not yet available at the time of this writing and is, therefore, not included in the phylogenies. Tree is rooted with Sunshine Coast Virus (GenBank accession number: YP_009094051.1) as an outgroup, with outgroup branch length shrunk for ease of viewing. Novel HNV, AngV, is depicted in green. Subfamilies and genera are demarcated, excluding those unassigned to subfamily (genera *Scolidonvirus*, *Cynoglossusvirus*, *Hoplichthysvirus*). Bootstrap support is depicted and GenBank accession numbers displayed next to virus names. Scale bar represents substitutions per site. (B) Time-resolved Bayesian phylogeny computed in BEAST 2 incorporating all available *Henipavirus* whole-genome nucleotide sequences, with the addition of newly discovered GAKV, DARV, and AngV. Closely related sequences are collapsed at triangle nodes for NiV and HeV (phylogeny with uncollapsed branches available in Fig. S2 in the supplemental material). HPD intervals of 95% around the timing of each branching node are visualized as red horizontal bars. Posterior support of >0.9 is indicated by black coloring of the corresponding node, and distinct *Henipavirus* species are indicated by colored tip points, with AngV highlighted in yellow for further emphasis. The estimated time to MRCA for Angavokely virus and the previously described bat-borne HNVs is 9,794 (95% HPD 6,519 to 14,025) years ago.

In N, P, C, V, W, M, and G amino acid phylogenies, the AngV proteins cluster closely with those of other HNVs (Fig. S3). Interestingly, in the amino acid phylogeny, the AngV F protein, like the F proteins of MojV, GAKV, and DARV, localizes ancestral to non-HNV paramyxoviruses and distinct from the bat-borne HNV clade (Fig. S3). The AngV L protein shows the

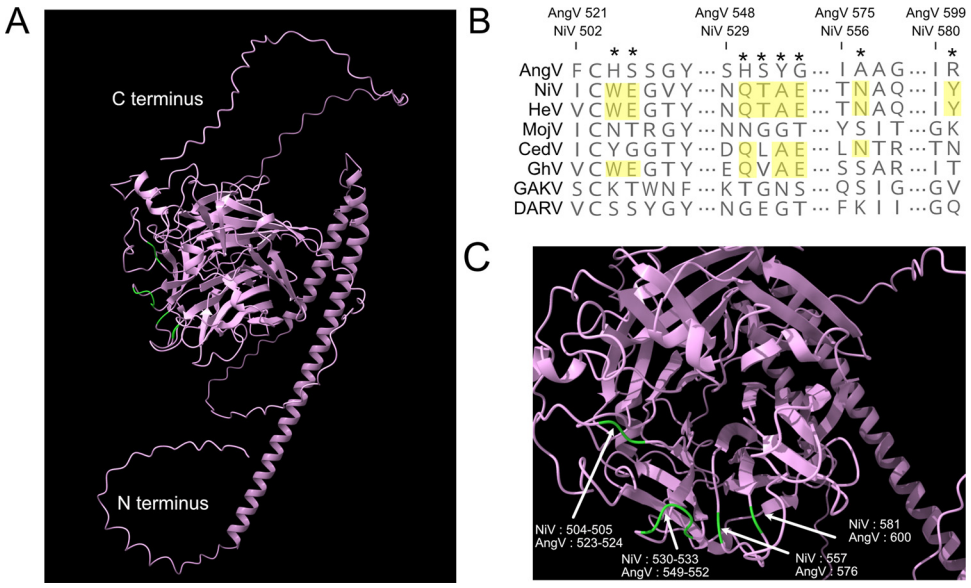

FIG 5 AlphaFold-predicted AngV glycoprotein 3D structure and ephrin binding residue sequence alignment. (A) AlphaFold-predicted 3D structure of AngV glycoprotein. N and C termini are indicated in white text, and residues corresponding to ephrin binding sites in other HNVs that are not conserved in AngV are colored green. (B) Alignment of HNV ephrin binding residues. The position of previously described HNV ephrin binding residues are noted by a star, and residues conserved across most HNVs are highlighted in yellow. Amino acid position numbers displayed represent the position within the AngV or NiV glycoproteins. Virus name (abbreviations) followed by GenBank accession number: Angavokely virus (AngV) ON613535; Nipah virus (NiV) AF212302; Hendra virus (HeV) AF017149; Mojiang virus (MojV) KF278639; Cedar virus (CedV) JQ001776; Ghanaian bat Henipavirus (GhV) HQ660129; Gamak virus (GAKV) MZ574407; Daeryong virus (DARV) MZ574409. (C) AlphaFold detail from full structure prediction for AngV. Localization of ephrin binding sites conserved across most HNVs is colored green and labeled corresponding to position in the NiV and AngV genomes.

highest amino acid identity to the L protein of rodent-borne Mount Mabu Lophuromys virus 2 (MMLV-2), a putative *Jeilongvirus* (23), but is nonetheless nested between the MojV/GAKV/DARV clade and the bat-borne HNV clade (Fig. S3).

AngV glycoprotein. We further examined the AngV G protein for conserved structural features and amino acid residues historically associated with HNV ephrin binding. AlphaFold analysis predicted a six-bladed β-propeller fold that is characteristic of *Paramyxoviridae* glycoproteins, with each blade largely composed of 4 antiparallel β-strands (Fig. 5A). The β-propeller fold is stabilized by seven disulfide bonds that are conserved among HNVs (Fig. S4). This HNV protein G structure-based alignment reveals that the elongated AngV G protein primarily results from a lengthy C-terminal tail with an additional 67 aa beyond that of NiV G protein (Fig. S4). Similar to the MojV G protein, the AngV G protein lacks previously described ephrin binding residues (NiV W504, E505, Q530, T531, A532, E533, N557, and Y581) (Fig. 5B and C; Fig. S4) (17, 24, 25).

DISCUSSION

We describe and characterize a novel HNV, AngV, from a urine sample collected from an *E. dupreanum* Malagasy fruit bat. In this study, urine samples from 206 unique fruit bats were assessed by metagenomic sequencing, yielding an overall positive HNV detection rate of 4.9% (10/206) for all bats studied and an HNV prevalence of 9.4% (10/106) for the *E. dupreanum* hosts. Of all the HNV positive samples, only one sample yielded sufficient reads for assembly of a complete coding sequence and subsequent genomic analysis. In a 6-year collection period spanning multiple wet/dry seasons, HNV-positive samples were only recovered from *E. dupreanum* bats in the Angavokely roosting site, despite prior serological evidence of HNV infection in *P. rufus* and *R. madagascariensis* bats, as well (22). HNV RNA was recovered from *E. dupreanum* in both wet and dry seasons, though higher sampling intensity throughout the wet season precludes any conclusions regarding underlying seasonal patterns in these data.

Previous work in this system has suggested a seasonal increase in fruit bat seroprevalence across the winter low-nutrient season, which also overlaps the gestation period for these synchronously breeding fruit bats (22). In fruit bat systems elsewhere, HNVs are also shed in urine at higher rates during the nutrient-poor dry seasons for the localities in question (26 to 28); in the case of NiV and HeV, these seasonal viral shedding pulses have been linked to zoonotic spillover.

The recovered genome of AngV exhibits a structural organization characteristic of the *Henipavirus* genus and a nucleotide and amino acid identity to HeV and NiV that is comparable to those shared with the more distantly related HNVs, MojV, GhV, and CedV. A limited quantity of available original sample precluded full genome recovery for AngV (as evidenced by the lack of the 5′ UTR region of the N ORF), which prevented analysis of the extent to which the full AngV genome may abide by the "rule of six," observed by all other members of the *Orthoparamyxovirinae* subfamily (29). Phylogenetic analyses of AngV support classification of this virus as a distinct novel bat-borne *Henipavirus* (L gene amino acid distance $<$0.82 distance for the subfamily *Orthoparamyxovirinae*), in accordance with the International Committee on Taxonomy of Viruses (ICTV) criteria (20). This novel HNV is estimated to have diverged approximately 9,800 years ago, prior to the currently known African and Asian bat-borne HNV lineages but considerably more recently than the estimated mid- to late-Miocene divergence of *E. dupreanum* from its sister species, *E. helvum*, on the African continent (30). Recent characterization of *Betacoronaviruses* in Madagascar fruit bats demonstrates surprising identity to lineages circulating in West Africa (31), suggesting that, though resident only in Madagascar, Malagasy fruit bats likely experience some form of contact with the African continent. Of the 49 bat species that inhabit the island nation of Madagascar, nine species are widely distributed across Africa, Asia, and/or Europe, presenting opportunities for interspecies viral transmission via island-hopping. Intensified viral sampling of Madagascar's insectivorous bat populations for HNVs thus represents an important future research priority.

As an ancestral bat-borne HNV, AngV may provide important insight into HNV evolution and pathogenesis. Similar to other paramyxoviruses, the encoded AngV P gene is able to produce multiple immunomodulatory protein products (32). One such protein product is the V protein, thought to be involved in immune evasion and considered a significant determinant of viral pathogenicity and lethality (33, 34). AngV harbors the highly conserved mRNA editing site and a predicted ORF that encodes a V protein with a conserved cysteine-rich C terminus, suggesting that AngV has the capacity to produce a functional V protein. With the exception of the newly discovered HNVs in shrews, GAKV and DARV, all HNVs harboring a V protein have previously demonstrated evidence of human infection, highlighting the potential for AngV to cause productive infection in humans (1, 9, 13). Further studies are needed to ascertain the virulence potential and host breadth of this novel virus.

Characterization of the AngV glycoprotein (G) through AlphaFold modeling and structure-based alignments revealed a similar structural organization to other HNV glycoproteins. Notably, the AngV glycoprotein surpasses that of GhV as the longest glycoprotein of the *Henipavirus* genus. Like that of GhV, the AngV glycoprotein harbors a long C-terminal extension (Fig. S4). It is unclear if the C-terminal extension of the AngV glycoprotein has a functional role, though the C-terminal extension of the glycoprotein in GhV is known to play a functional role in receptor-mediated fusion (16).

Henipavirus host tropism and virulence rely on a myriad of factors, one of which is the HNV glycoprotein. The previously characterized HNV glycoproteins of NiV, HeV, CedV, and GhV utilize members of the ephrinA and ephrinB class family as host-cell receptors for viral entry into human cells (16 to 18, 24, 35). However, like MojV, the AngV glycoprotein lacks these well-conserved ephrin binding residues. Structure-based alignments can shed light on potential receptor binding residues when characterizing novel viruses. For instance, sequence-based comparisons of the GhV and NiV glycoproteins were used to predict GhV ephrin binding (13), which was later confirmed by crystallography (16). Structure-based alignment of the AngV glycoprotein shows a lack of

highly conserved ephrin binding residues, including NiV E533—a seminal residue for ephrinB2 binding that is conserved across all ephrin binding HNVs. This suggests that, like MojV—and probably DARV, GAKV, and LayV—the AngV glycoprotein may not bind ephrins, pointing to the possible use of an ancestral viral entry pathway. The growing number of novel HNVs that appear not to rely on ephrin binding for cellular entry could warrant reevaluation of the existing HNV genus to better reflect conserved function and pathobiology.

This work presents a novel bat-HNV, AngV, identified from a Malagasy fruit bat. AngV joins a growing group of ancestral HNVs with unknown cell-entry receptors. Discovery of the cell surface receptor for AngV represents an important future research priority that will shed light on the breadth of host range for this virus, including its zoonotic potential.

MATERIALS AND METHODS

Ethics statement. Animal capture and handling and subsequent collection of biological samples were conducted in strict accordance with the Madagascar Ministry of Forest and the Environment (permit numbers 019/18, 170/18, 007/19) and guidelines posted by the American Veterinary Medical Association. Field protocols were approved by the UC Berkeley Animal Care and Use Committee (ACUC Protocol number AUP-2017-10-10393), as previously described (31).

Animal capture, sample collection, and RNA extraction. Fruit bats were captured and processed in part with a long-term study investigating the seasonal dynamics of potentially zoonotic viruses in Madagascar, as has been previously described (22, 31, 36 to 38). Animals were identified morphologically by species, sex, and age class (juvenile versus adult), and urine swabs were collected into a viral transport medium from any individual that urinated during handling. Urine swabs were flash-frozen in liquid nitrogen in the field and delivered to −80°C freezers at Institut Pasteur de Madagascar for long-term storage. Urine specimens from 206 bats were randomly selected for total RNA extraction using the Zymo Quick RNA/DNA Microprep Plus kit, performed as previously described (31).

mNGS library preparation. Total urine RNAs were diluted with nuclease-free H_2O, and 5 μL of each specimen was used as input for mNGS library preparation. A 2-fold dilution series of a 25-ng/μL stock of HeLa total RNA (n = 8 samples), along with 5 water samples, were included and processed in parallel as positive and negative controls, respectively. Additionally, a 25-pg aliquot of External RNA Control Consortium (ERCC) spike-in mix (Thermo-Fisher) was included in each sample. Dual-indexed mNGS library preparations for the samples were miniaturized and performed in 384-well format with NEBNext Ultra II RNAseq library preparation kit (New England Biolabs) reagents. RNA samples were fragmented for 12 min at 94°C, and 16 cycles of PCR amplification were performed. Per-sample read yields from a small-scale iSeq (Illumina) paired-end 2 × 146 bp sequencing run on an equivolume pool of the individual libraries were used to normalize volumes of the individual mNGS libraries to generate an equimolar pool. Paired-end 2 × 146 bp sequencing of the resulting equimolar library pool was performed on the NovaSeq6000 (Illumina) to obtain approximately 50 million reads per sample.

Sequence analysis. Raw reads from urine sample sequencing were first uploaded to the CZBID (v.6.8) platform for host and quality filtering and *de novo* assembly (39). In brief, in the CZBID pipeline, adaptor sequences were removed with Trimmomatic (v.0.38), and reads were quality filtered (40). Reads then underwent host filtration against the Malagasy fruit bat genome, *E. dupreanum*, using STAR (v.2.7.9a) (41) and a second host-removal step using Bowtie2 (42). After host filtering, reads were aligned using RAPSearch2 (43) and GSNAP (44), and putative pathogen taxa were identified. Next, reads were assembled using SPADES (v.3.15.3) (45), and all contigs generated were subject to BLAST analysis against the putative taxa previously identified by RAPSearch2 and GSNAP. We considered samples positive for HNV if the CZBID pipeline produced at least one contig with an average read depth of two or more, which yielded a BLAST alignment length of >100 nt/aa and an E value of <0.00001 (BLASTn v.2.5.0+) or a bit score of >100 (BLASTx v.2.5.0+) when queried against an HNV database derived from all HNV genomes available in NCBI (accessed July 2021).

Genome annotation and comparison. One urine sample, collected from an adult female *E. dupreanum* fruit bat in March 2019, yielded a near full-length HNV genome, which we analyzed in greater depth in subsequent analyses and annotated as the novel HNV, AngV (GenBank accession number: ON613535). Nucleotide BLAST of the AngV genome identified NiV (GenBank accession number: AF212302) as the top hit for this novel virus and was subsequently chosen as the reference genome for further analysis. We aligned AngV to NiV (GenBank accession number: AF212302) in the program Geneious Prime (v.2020.2.4) and annotated all six major HNV structural genes, and the accessory C ORF, within the P gene. We identified the putative mRNA editing site within the P gene sequence (spanning nucleotides 1,225 to 1,232 of the P gene) and manually added one or two guanine (G) residues to the 3′ end of the conserved HNV mRNA editing site to generate V and W ORFs, respectively, and their corresponding proteins. We furthered queried all identified transcriptional elements against publicly available sequences using NCBI BLAST and BLASTx (46). Resulting BLAST and BLASTx hits were used in phylogenetic analyses as described below.

We used the program pySimPlot to scan the whole-genome sequence of AngV for nucleotide sequence identity to the NiV genome (GenBank accession number: AF212302) and the nucleotide and amino acid sequences of individual open reading frames (ORFs) contained therein. Respectively, window size and

scanning were specified as 50 and 1 for nucleotide pairwise identity and 50 and 5 for amino acid pairwise identity. Results were visualized using Prism (9.2.0).

Phylogenetic analyses. We constructed 10 maximum likelihood (ML) amino acid phylogenies to analyze the evolutionary relatedness of our putative HNV to previously described paramyxoviruses. We note that the sequence for the newly described LayV was not yet available at the time of this writing and is, therefore, absent from all phylogenies. Our first ML phylogeny compared the translated L protein of AngV to all translated reference L protein paramyxovirus sequences in NCBI, in addition to those of the newly described shrew HNVs, GAKV and DARV (accessed November 2021). The nine subsequent ML phylogenies compared the translation of each individual protein annotated for AngV (N, P, C, V, W, M, F, G, L) against the top 50 BLASTx sequence hits for each protein collapsed on 98% similarity. Distinct outgroups were applied: (i) Sunshine Coast Virus (GenBank accession number: YP_009094051.1) for the first L protein phylogeny, (ii) human orthopneumovirus (HRSV, GenBank accession number: NC_001781) for N, P, M, F, G, and L proteins, and (iii) Sendai virus (GenBank accession number:
NP_056872) for gene C.

For each phylogenetic tree, we aligned translated amino acid sequences via the MUSCLE algorithm (v.3.8.1551) (47) and determined the best fit amino acid substitution model using ModelTest-NG (48). Phylogenies were then constructed in RAxML-NG (49), using the corresponding best fit model: JTT (complete L-protein sequence) or LG+G4+F (individual proteins). In accordance with best practices outlined in the RAxML-NG manual, 20 ML inferences were made on each original alignment. Bootstrap replicate trees were inferred using Felsenstein's method (50). MRE-based bootstrapping test was applied after every 200 replicates (51), and bootstrapping was terminated once diagnostic statistics dropped below the threshold value. Bootstrap support values were drawn on the best-scoring tree.

We additionally computed one Bayesian time-resolved phylogeny, using all 77 full-length HNV nucleotide sequences available in NCBI, including our newly contributed AngV (GenBank accession number: ON613535). As with ML trees, sequences were first aligned in MUSCLE (v.3.8.1551) (47), and the best-fit nucleotide substitution model was subsequently queried in ModelTest-NG (48). We then constructed a Bayesian timetree in the program BEAST 2 (52, 53), using the best-fit GTR+I+G4 model inferred for the whole-genome alignment from ModelTest-NG and assuming a constant population prior. Sampling dates corresponded to collection data as reported in NCBI Virus; we assumed a collection date of 31 July in cases where only year of collection was reported. We computed trees using both an uncorrelated exponentially distributed relaxed molecular clock (UCED) and a strict clock but here report results from the strict clock only as similar results were inferred from both. We ran Markov Chain Monte Carlo (MCMC) sample chains for 1 billion iterations, checked convergence using TRACER v.1.7 (54), and averaged trees after 10% burn-in using TreeAnnotator v.2.6.3 (55) to visualize mean posterior densities at each node. The resulting phylogeny was visualized in R v.4.0.3 for MacIntosh in the "ggtree" package (56).

AngV G protein structure modeling. We used the artificial intelligence system AlphaFold to predict the 3D structure of the AngV glycoprotein (G) (57). Molecular graphics and analyses of the AngV glycoprotein structure were performed with UCSF ChimeraX (58). HNV glycoprotein ephrin binding residues were aligned using the program Geneious Prime (v.2020.2.4).

Data availability. Raw and assembled sequencing data are deposited in NCBI BioProject PRJNA837298. The full genome of AngV is available in GenBank under accession number ON613535. All raw data and code for figures can be obtained in our open-access GitHub repository: https://github.com/brooklabteam/angavokely-virus.

SUPPLEMENTAL MATERIAL

Supplemental material is available online only.

SUPPLEMENTAL FILE 1, PDF file, 2.5 MB.

ACKNOWLEDGMENTS

We thank Anecia Gentles and Kimberly Rivera for help in the field and the lab and acknowledge the Virology Unit at the Institut Pasteur de Madagascar and Maira Phelps of the Chan Zuckerberg Biohub (CZB) for logistical support. We additionally thank Angela Detweiler, Michelle Tan, and Norma Neff of the CZB genomics platform for mNGS support. Molecular graphics and analyses were performed with UCSF ChimeraX, developed by the Resource for Biocomputing, Visualization, and Informatics at the University of California, San Francisco, with support from the National Institutes of Health R01-GM129325 and the Office of Cyber Infrastructure and Computational Biology, National Institute of Allergy and Infectious Diseases.

This work was supported by the National Institutes of Health (1R01AI129822-01 grant to J.-M.H., P.D., and C.E.B.; 5T32AI007641-19 to S.M.; and R01AI109022 to H.C.A.), DARPA (PREEMPT Program Cooperative Agreement no. D18AC00031 to C.E.B.), the Bill and Melinda Gates Foundation (GCE/ID OPP1211841 to C.E.B. and J.-M.H.), the Adolph C. and Mary Sprague Miller Institute for Basic Research in Science (postdoctoral fellowship

to C.E.B.), AAAS/L'Oréal USA (For Women in Science fellowship to C.E.B.), the Branco Weiss Society in Science (fellowship to C.E.B.), and the Chan Zuckerberg Biohub.

We declare no competing interests.

REFERENCES

1. Eaton BT, Broder CC, Middleton D, Wang L-F. 2006. Hendra and Nipah viruses: different and dangerous. Nat Rev Microbiol 4:23–35. https://doi.org/10.1038/nrmicro1323.
2. Sharma V, Kaushik S, Kumar R, Yadav JP, Kaushik S. 2019. Emerging trends of Nipah virus: a review. Rev Med Virol 29:e2010. https://doi.org/10.1002/rmv.2010.
3. Arunkumar G, Chandni R, Mourya DT, Singh SK, Sadanandan R, Sudan P, Bhargava B, Nipah Investigators People and Health Study Group. 2019. Outbreak investigation of Nipah virus disease in Kerala, India, 2018. J Infect Dis 219:1867–1878. https://doi.org/10.1093/infdis/jiy612.
4. Murray K, Selleck P, Hooper P, Hyatt a, Gould a, Gleeson L, Westbury H, Hiley L, Selvey L, Rodwell B. 1995. A morbillivirus that caused fatal disease in horses and humans. Science 268:94–97. https://doi.org/10.1126/science.7701348.
5. Hsu VP, Hossain MJ, Parashar UD, Ali MM, Ksiazek TG, Kuzmin I, Niezgoda M, Rupprecht C, Bresee J, Breiman RF. 2004. Nipah virus encephalitis reemergence, Bangladesh. Emerg Infect Dis 10:2082–2087. https://doi.org/10.3201/eid1012.040701.
6. Gurley ES, Montgomery JM, Hossain MJ, Bell M, Azad AK, Islam MR, Molla MAR, Carroll DS, Ksiazek TG, Rota PA, Lowe L, Comer JA, Rollin P, Czub M, Grolla A, Feldmann H, Luby SP, Woodward JL, Breiman RF. 2007. Person-to-Person transmission of Nipah virus in a Bangladeshi community. Emerg Infect Dis 13:1031–1037. https://doi.org/10.3201/eid1307.061128.
7. Luby SP, Gurley ES. 2012. Epidemiology of henipavirus disease in humans, p 25–40. *In* Lee B, Rota PA (ed), Henipavirus. Springer Berlin Heidelberg, Berlin, Germany.
8. Marsh GA, de Jong C, Barr JA, Tachedjian M, Smith C, Middleton D, Yu M, Todd S, Foord AJ, Haring V, Payne J, Robinson R, Broz I, Crameri G, Field HE, Wang L-F. 2012. Cedar virus: a novel henipavirus isolated from Australian bats. PLoS Pathog 8:e1002836. https://doi.org/10.1371/journal.ppat.1002836.
9. Wu Z, Yang L, Yang F, Ren X, Jiang J, Dong J, Sun L, Zhu Y, Zhou H, Jin Q. 2014. Novel henipa-like virus, *Mojiang paramyxovirus*, in rats, China, 2012. Emerg Infect Dis 20:1064–1066. https://doi.org/10.3201/eid2006.131022.
10. Lee SH, Kim K, Kim J, No JS, Park K, Budhathoki S, Lee SH, Lee J, Cho SH, Cho S, Lee GY, Hwang J, Kim HC, Klein TA, Uhm CS, Kim WK, Song JW. 2021. Discovery and genetic characterization of novel paramyxoviruses related to the genus *Henipavirus* in *Crocidura* species in the republic of Korea. Viruses 13:2020. https://doi.org/10.3390/v13102020.
11. Drexler JF, Corman VM, Müller MA, Maganga GD, Vallo P, Binger T, Gloza-Rausch F, Cottontail VM, Rasche A, Yordanov S, Seebens A, Knörnschild M, Oppong S, Adu Sarkodie Y, Pongombo C, Lukashev AN, Schmidt-Chanasit J, Stöcker A, Carneiro AJB, Erbar S, Maisner A, Fronhoffs F, Buettner R, Kalko EKV, Kruppa T, Franke CR, Kallies R, Yandoko ERN, Herrler G, Reusken C, Hassanin A, Krüger DH, Matthee S, Ulrich RG, Leroy EM, Drosten C. 2012. Bats host major mammalian paramyxoviruses. Nat Commun 3:796. https://doi.org/10.1038/ncomms1796.
12. Zhang X-A, Li H, Jiang F-C, Zhu F, Zhang Y-F, Chen J-J, Tan C-W, Anderson DE, Fan H, Dong L-Y, Li C, Zhang P-H, Li Y, Ding H, Fang L-Q, Wang L-F, Liu W. 2022. A zoonotic henipavirus in febrile patients in China. N Engl J Med 387:470–470. https://doi.org/10.1056/NEJMc2202705.
13. Pernet O, Schneider BS, Beaty SM, LeBreton M, Yun TE, Park A, Zachariah TT, Bowden TA, Hitchens P, Ramirez CM, Daszak P, Mazet J, Freiberg AN, Wolfe ND, Lee B. 2014. Evidence for henipavirus spillover into human populations in Africa. Nat Commun 5:5342. https://doi.org/10.1038/ncomms6342.
14. Amaya M, Broder CC. 2020. Vaccines to emerging viruses: Nipah and Hendra. Annu Rev Virol 7:447–473. https://doi.org/10.1146/annurev-virology-021920-113833.
15. Cheliout Da Silva S, Yan L, Dang H v, Xu K, Epstein JH, Veesler D, Broder CC. 2021. Functional analysis of the fusion and attachment glycoproteins of Mojiang henipavirus. Viruses 13:517. https://doi.org/10.3390/v13030517.
16. Lee B, Pernet O, Ahmed AA, Zeltina A, Beaty SM, Bowden TA. 2015. Molecular recognition of human ephrinB2 cell surface receptor by an emergent African henipavirus. Proc Natl Acad Sci U S A 112:E2156–E2165. https://doi.org/10.1073/pnas.1501690112.
17. Laing ED, Navaratnarajah CK, Cheliout Da Silva S, Petzing SR, Xu Y, Sterling SL, Marsh GA, Wang L-F, Amaya M, Nikolov DB, Cattaneo R, Broder CC, Xu K. 2019. Structural and functional analyses reveal promiscuous and species specific use of ephrin receptors by Cedar virus. Proc Natl Acad Sci U S A 116:20707–20715. https://doi.org/10.1073/pnas.1911773116.
18. Rissanen I, Ahmed AA, Azarm K, Beaty S, Hong P, Nambulli S, Duprex WP, Lee B, Bowden TA. 2017. Idiosyncratic Mòjiang virus attachment glycoprotein directs a host-cell entry pathway distinct from genetically related henipaviruses. Nat Commun 8:16060. https://doi.org/10.1038/ncomms16060.
19. Flick R, Walpita P, Czub M, Guerrant RL, Walker DH, Weller PF. 2006. Nipah and Hendra viral infections, p 586–589. *In* Tropical infectious diseases. Churchill Livingstone, London, United Kingdom.
20. Rima B, Buschmann AB, Dundon WG, Duprex P, Easton A, Fouchier R, Kurath G, Lamb R, Lee B, Rota P, Wang L, ICTV Report Consortium. 2019. ICTV virus taxonomy profile: *Paramyxoviridae*. J Gen Virol 100:1593–1594. https://doi.org/10.1099/jgv.0.001328.
21. Calain P, Roux L. 1993. The rule of six, a basic feature for efficient replication of Sendai virus defective interfering RNA. J Virol 67:4822–4830. https://doi.org/10.1128/JVI.67.8.4822-4830.1993.
22. Brook CE, Ranaivoson HC, Broder CC, Cunningham AA, Héraud J-M, Peel AJ, Gibson L, Wood JLN, Metcalf CJ, Dobson AP. 2019. Disentangling serology to elucidate henipa- and filovirus transmission in Madagascar fruit bats. J Anim Ecol 88:1001–1016. https://doi.org/10.1111/1365-2656.12985.
23. Vanmechelen B, Bletsa M, Laenen L, Lopes AR, Vergote V, Beller L, Deboutte W, Korva M, Avšič Županc T, Goüy de Bellocq J, Gryseels S, Leirs H, Lemey P, Vrancken B, Maes P. 2018. Discovery and genome characterization of three new Jeilongviruses, a lineage of paramyxoviruses characterized by their unique membrane proteins. BMC Genomics 19:617. https://doi.org/10.1186/s12864-018-4995-0.
24. Guillaume V, Aslan H, Ainouze M, Guerbois M, Fabian Wild T, Buckland R, Langedijk JPM. 2006. Evidence of a potential receptor-binding site on the Nipah virus G protein (NiV-G): identification of globular head residues with a role in fusion promotion and their localization on an NiV-G structural model. J Virol 80:7546–7554. https://doi.org/10.1128/JVI.00190-06.
25. Negrete OA, Wolf MC, Aguilar HC, Enterlein S, Wang W, Mühlberger E, Su S, Bertolotti-Ciarlet A, Flick R, Lee B. 2006. Two key residues in ephrinB3 are critical for its use as an alternative receptor for Nipah virus. PLoS Pathog 2:e7. https://doi.org/10.1371/journal.ppat.0020007.
26. Field H, Jordan D, Edson D, Morris S, Melville D, Parry-Jones K, Broos A, Divljan A, McMichael L, Davis R, Kung N, Kirkland P, Smith C. 2015. Spatiotemporal aspects of Hendra virus infection in pteropid bats (flying-foxes) in Eastern Australia. PLoS One 10:e0144055. https://doi.org/10.1371/journal.pone.0144055.
27. Páez DJ, Giles J, Mccallum H, Field H, Jordan D, Peel AJ, Plowright RK. 2017. Conditions affecting the timing and magnitude of Hendra virus shedding across pteropodid bat populations in Australia. Epidemiol Infect 145:3143–3153. https://doi.org/10.1017/S0950268817002138.
28. Cappelle J, Furey N, Hoem T, Ou TP, Lim T, Hul V, Heng O, Chevalier V, Dussart P, Duong V. 2021. Longitudinal monitoring in Cambodia suggests higher circulation of alpha and betacoronaviruses in juvenile and immature bats of three species. Sci Rep 11:24145. https://doi.org/10.1038/s41598-021-03169-z.
29. Hausmann S, Jacques J-P, Kolakofsky D. 1996. Paramyxovirus RNA editing and the requirement for hexamer genome length. RNA 2:1033–1045.
30. Shi JJ, Chan LM, Peel AJ, Lai R, Yoder AD, Goodman SM. 2014. A deep divergence time between sister species of *Eidolon* (Pteropodidae) with evidence for widespread panmixia. Acta Chiropterologica 16:279–292. https://doi.org/10.3161/150811014X687242.
31. Kettenburg G, Kistler A, Ranaivoson HC, Ahyong V, Andrianiaina A, Andry S, DeRisi JL, Gentles A, Raharinosy V, Randriambolamanantsoa TH, Ravelomanantsoa NAF, Tato CM, Dussart P, Heraud J-M, Brook CE. 2022. Full genome *Nobecovirus* sequences from Malagasy fruit bats define a unique evolutionary history for this coronavirus clade. Front Public Health 10:786060. https://doi.org/10.3389/fpubh.2022.786060.
32. Douglas J, Drummond AJ, Kingston RL. 2021. Evolutionary history of cotranscriptional editing in the paramyxoviral phosphoprotein gene. Virus Evol 7:veab028. https://doi.org/10.1093/ve/veab028.

33. Satterfield BA, Cross RW, Fenton KA, Agans KN, Basler CF, Geisbert TW, Mire CE. 2015. The immunomodulating V and W proteins of Nipah virus determine disease course. Nat Commun 6:7483. https://doi.org/10.1038/ncomms8483.
34. Patterson JB, Thomas D, Lewicki H, Billeter MA, Oldstone MBA. 2000. V and C proteins of measles virus function as virulence factors in vivo. Virology 267:80–89. https://doi.org/10.1006/viro.1999.0118.
35. Negrete OA, Chu D, Aguilar HC, Lee B. 2007. Single amino acid changes in the Nipah and Hendra virus attachment glycoproteins distinguish ephrinB2 from ephrinB3 usage. J Virol 81:10804–10814. https://doi.org/10.1128/JVI.00999-07.
36. Brook CE, Ranaivoson HC, Andriafidison D, Ralisata M, Razafimanahaka J, Héraud J, Dobson AP, Metcalf CJ. 2019. Population trends for two Malagasy fruit bats. Biol Conserv 234:165–171. https://doi.org/10.1016/j.biocon.2019.03.032.
37. Ranaivoson HC, Héraud J-M, Goethert HK, Telford SR, III, Rabetafika L, Brook CE. 2019. Babesial infection in the Madagascan flying fox, *Pteropus rufus* É. Geoffroy, 1803. Parasit Vectors 12:51. https://doi.org/10.1186/s13071-019-3300-7.
38. Brook CE, Bai Y, Dobson AP, Osikowicz LM, Ranaivoson HC, Zhu Q, Kosoy MY, Dittmar K. 2015. *Bartonella* spp. in fruit bats and blood-feeding ectoparasites in Madagascar. PLoS Negl Trop Dis 9:e0003532. https://doi.org/10.1371/journal.pntd.0003532.
39. Kalantar KL, Carvalho T, de Bourcy CFA, Dimitrov B, Dingle G, Egger R, Han J, Holmes OB, Juan YF, King R, Kislyuk A, Lin MF, Mariano M, Morse T, Reynoso L, Cruz DR, Sheu J, Tang J, Wang J, Zhang MA, Zhong E, Ahyong V, Lay S, Chea S, Bohl JA, Manning JE, Tato CM, DeRisi JL. 2020. IDseq—an open source cloud-based pipeline and analysis service for metagenomic pathogen detection and monitoring. Gigascience 9:giaa111. https://doi.org/10.1093/gigascience/giaa111.
40. Bolger AM, Lohse M, Usadel B. 2014. Trimmomatic: a flexible trimmer for Illumina sequence data. Bioinformatics 30:2114–2120. https://doi.org/10.1093/bioinformatics/btu170.
41. Dobin A, Davis CA, Schlesinger F, Drenkow J, Zaleski C, Jha S, Batut P, Chaisson M, Gingeras TR. 2013. STAR: ultrafast universal RNA-seq aligner. Bioinformatics 29:15–21. https://doi.org/10.1093/bioinformatics/bts635.
42. Langmead B, Salzberg SL. 2012. Fast gapped-read alignment with Bowtie 2. Nat Methods 9:357–360. https://doi.org/10.1038/nmeth.1923.
43. Zhao Y, Tang H, Ye Y. 2012. RAPSearch2: a fast and memory-efficient protein similarity search tool for next-generation sequencing data. Bioinformatics 28:125–126. https://doi.org/10.1093/bioinformatics/btr595.
44. Wu TD, Nacu S. 2010. Fast and SNP-tolerant detection of complex variants and splicing in short reads. Bioinformatics 26:873–881. https://doi.org/10.1093/bioinformatics/btq057.
45. Bankevich A, Nurk S, Antipov D, Gurevich AA, Dvorkin M, Kulikov AS, Lesin VM, Nikolenko SI, Pham S, Prjibelski AD, Pyshkin AV, Sirotkin AV, Vyahhi N, Tesler G, Alekseyev MA, Pevzner PA. 2012. SPAdes: a new genome assembly algorithm and its applications to single-cell sequencing. J Comput Biol 19:455–477. https://doi.org/10.1089/cmb.2012.0021.
46. Altschul SF, Gish W, Miller W, Myers EW, Lipman DJ. 1990. Basic local alignment search tool. J Mol Biol 215:403–410. https://doi.org/10.1016/S0022-2836(05)80360-2.
47. Edgar RC. 2004. MUSCLE: multiple sequence alignment with high accuracy and high throughput. Nucleic Acids Res 32:1792–1797. https://doi.org/10.1093/nar/gkh340.
48. Darriba D, Posada D, Kozlov AM, Stamatakis A, Morel B, Flouri T. 2020. ModelTest-NG: a new and scalable tool for the selection of DNA and protein evolutionary models. Mol Biol Evol 37:291–294. https://doi.org/10.1093/molbev/msz189.
49. Kozlov AM, Darriba D, Flouri T, Morel B, Stamatakis A. 2019. RAxML-NG: a fast, scalable and user-friendly tool for maximum likelihood phylogenetic inference. Bioinformatics 35:4453–4455. https://doi.org/10.1093/bioinformatics/btz305.
50. Felsenstein J. 1985. Confidence limits on phylogenies: an approach using the bootstrap. Evolution 39:783–791. https://doi.org/10.2307/2408678.
51. Pattengale ND, Alipour M, Bininda-Emonds ORP, Moret BME, Stamatakis A. 2010. How many bootstrap replicates are necessary? J Comput Biol 17:337–354. https://doi.org/10.1089/cmb.2009.0179.
52. Bouckaert R, Heled J, Kühnert D, Vaughan T, Wu CH, Xie D, Suchard MA, Rambaut A, Drummond AJ. 2014. BEAST 2: a software platform for Bayesian evolutionary analysis. PLoS Comput Biol 10:e1003537. https://doi.org/10.1371/journal.pcbi.1003537.
53. Drummond AJ, Suchard MA, Xie D, Rambaut A. 2012. Bayesian phylogenetics with BEAUti and the BEAST 1.7. Mol Biol Evol 29:1969–1973. https://doi.org/10.1093/molbev/mss075.
54. Rambaut A, Drummond AJ, Xie D, Baele G, Suchard MA. 2018. Posterior summarization in Bayesian phylogenetics using Tracer 1.7. Syst Biol 67:901–904. https://doi.org/10.1093/sysbio/syy032.
55. Drummond AJ, Rambaut A. 2007. BEAST: Bayesian evolutionary analysis by sampling trees. BMC Evol Biol 7:214. https://doi.org/10.1186/1471-2148-7-214.
56. Yu G, Smith DK, Zhu H, Guan Y, Lam TTY. 2017. Ggtree: an R Package for visualization and annotation of phylogenetic trees with their covariates and other associated data. Methods Ecol Evol 8:28–36. https://doi.org/10.1111/2041-210X.12628.
57. Jumper J, Evans R, Pritzel A, Green T, Figurnov M, Ronneberger O, Tunyasuvunakool K, Bates R, Žídek A, Potapenko A, Bridgland A, Meyer C, Kohl SAA, Ballard AJ, Cowie A, Romera-Paredes B, Nikolov S, Jain R, Adler J, Back T, Petersen S, Reiman D, Clancy E, Zielinski M, Steinegger M, Pacholska M, Berghammer T, Bodenstein S, Silver D, Vinyals O, Senior AW, Kavukcuoglu K, Kohli P, Hassabis D. 2021. Highly accurate protein structure prediction with AlphaFold. Nature 596:583–589. https://doi.org/10.1038/s41586-021-03819-2.
58. Pettersen EF, Goddard TD, Huang CC, Meng EC, Couch GS, Croll TI, Morris JH, Ferrin TE. 2021. UCSF ChimeraX: structure visualization for researchers, educators, and developers. Protein Sci 30:70–82. https://doi.org/10.1002/pro.3943.